

# Bar-Driven Galaxy Evolution at Intermediate Redshifts

Shardha Jogee<sup>1</sup>, Johan H. Knapen<sup>2</sup>, Isaac Shlosman<sup>3</sup>, Gabriel Lubell<sup>4</sup>, James Davies<sup>1</sup>, Marco Barden<sup>5</sup>, Steven V. W. Beckwith<sup>1</sup>, Eric F. Bell<sup>5</sup>, Andrea Borch<sup>5</sup>, John A. R. Caldwell<sup>1</sup>, Boris Häußler<sup>5</sup>, Knud Jahnke<sup>6</sup>, Daniel H. McIntosh<sup>7</sup>, Klaus Meisenheimer<sup>5</sup>, Chien Y. Peng<sup>8</sup>, Hans-Walter Rix<sup>5</sup>, Sebastian F. Sanchez<sup>6</sup>, Rachel S. Somerville<sup>1</sup>, Lutz Wisotzki<sup>6</sup>, Christian Wolf<sup>9</sup>, Chris Conselice<sup>10</sup>, Seppo Laine<sup>10</sup>, Swara Ravindranath<sup>1</sup>, Bahram Mobasher<sup>1</sup>

1=Space Telescope Science Institute, USA 2=University of Hertfordshire, UK 3=University of Kentucky, USA 4=Vassar College, USA 5=Max-Planck Institute for Astronomy, Germany 6=Astrophysikalisches Institut Potsdam, Germany 7=University of Massachusetts, USA 8=University of Arizona, USA 9=Oxford University, UK 10=California Institute of Technology, USA;

**SUMMARY:** Non-axisymmetric features such as spontaneous and induced bars drive the dynamical and secular evolution of disk galaxies by exerting gravitational torques which redistribute mass and angular momentum. While most (> 70 %) spirals are barred in the local Universe, early studies of the Hubble Deep Field (HDF) suggest a remarkably low bar fraction (< 20%) at intermediate redshifts ( $z=0.5-0.8$ ). If confirmed, this result would imply that disks at these epochs are fundamentally different from present-day spirals. We revisit the recoverability, fraction, and properties of bars at intermediate redshifts using the two largest HST surveys to date: Galaxy Evolution from Morphology and SEDs (GEMS) and the Great Observatories Origins Deep Survey (GOODS). We also present first results to analyze the stability of bars embedded in massive halos of various central concentrations and asymmetries.

## HOW WELL CAN WE RECOVER BARS AT $Z \sim 1$ ?

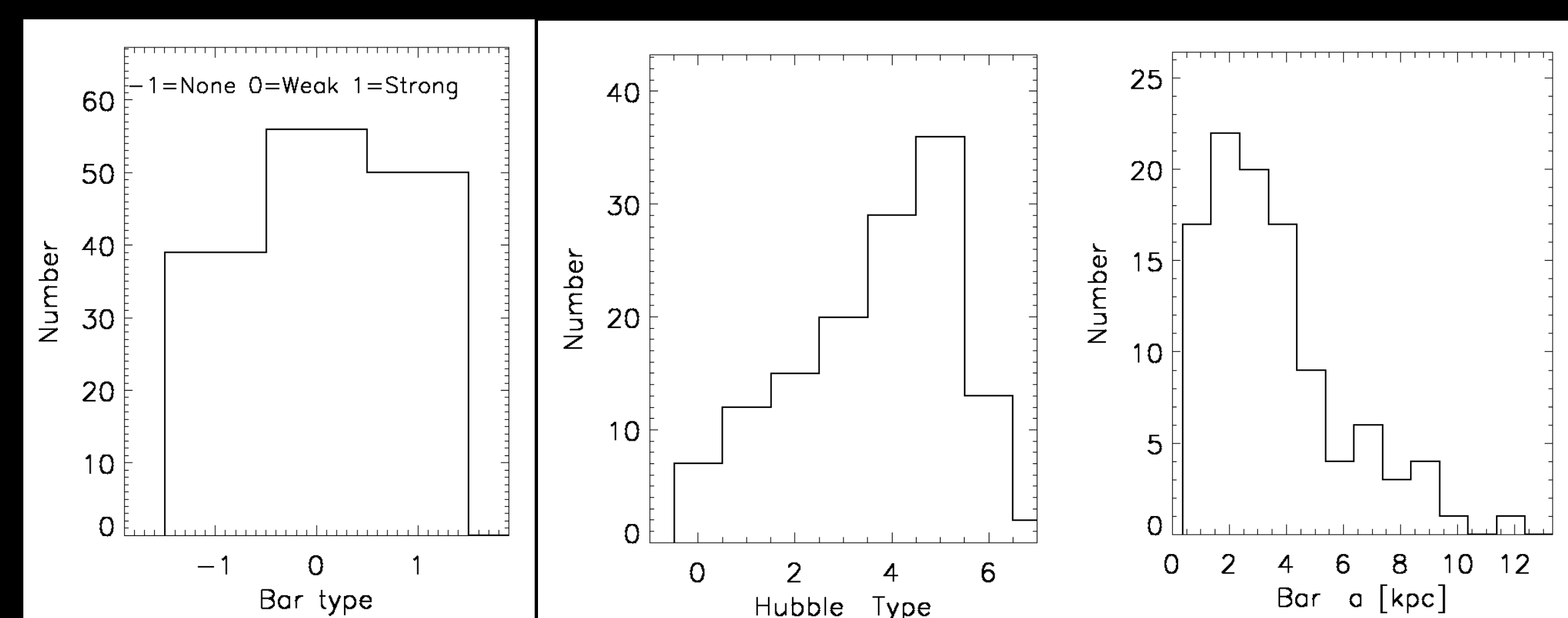


FIG. 1 - The local sample of 144 bright moderately inclined spiral galaxies used in our simulations has a bar fraction (72%; left), Hubble types (middle), and bar sizes (right) representative of the local Universe.

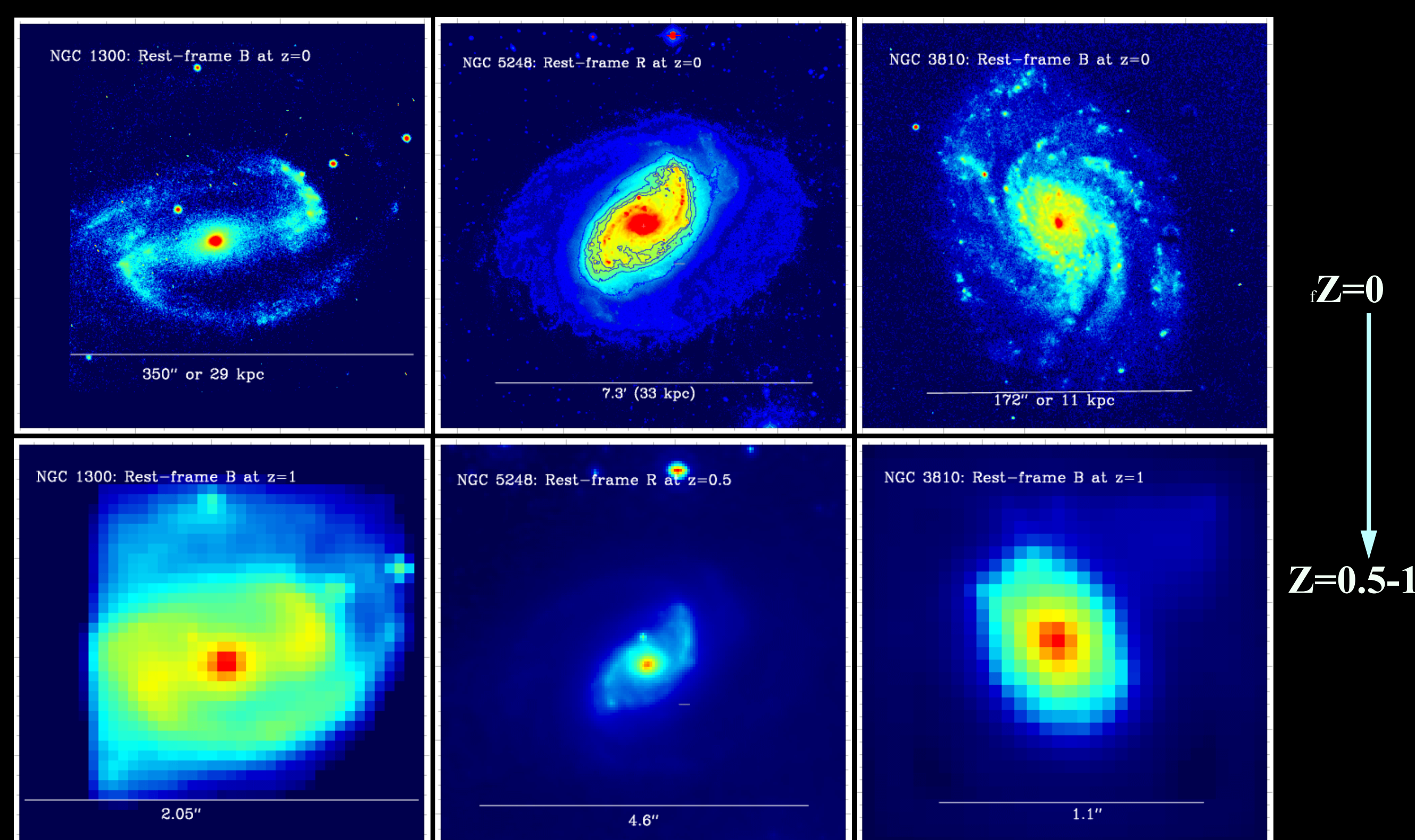


FIG. 2 - Recoverability of bars from our simulations: **Left:** Extended strong bars can be recovered even out to  $z=1$ . **Middle:** For systems with faint disks and weak bars hosting spiral patterns of star formation, cosmological dimming can fade the outer disk beyond detection and cause the inner weak bar to be misidentified as a disk (Jogee et al. 2002). **Right:** Due to the loss of spatial resolution, short bars ( $a < 3-4$  kpc) are washed out into diffuse inner disks implying that only large bars (which make up only a small fraction of local bars - see Fig. 1) can be recovered in ACS surveys at intermediate redshifts (Jogee et al. 2003). This bias is even more pronounced in WFC2 and NICMOS data (e.g., Sheth et al. 2003)

- **GEMS** (Rix et al. 2003) is a large-area ( $30' \times 30'$  or 150 Hubble Deep Field Areas), deep HST ACS 2-color (F606W, F850LP) survey centered on the Chandra Deep Field South (CDF-S). It focuses on galaxy evolution out to a redshift of 1.2 where the Universe was half of its present age. Redshifts and SEDs for 10,000 galaxies are available from the ground-based COMBO-17 survey (Wolf et al. 2003).
- **GOODS** (Giavalisco et al. 2003) consists of deep HST ACS 4-color (F435W, F606W, F775W, F850LP) images, ground-based optical and NIR data, and planned SIRTf observations from 3.6-24 micron over two  $16' \times 10'$  fields centered on the CDF-S and the HDF-N.
- GEMS and GOODS HST data trace the rest-frame B and R light out to  $z \sim 1.2$  and  $z \sim 0.5$ , respectively. The data have better resolution, a factor of  $>10$  improvement in number statistics, and redder wavelength coverage compared to the WFC2 HDF data used in earlier studies. The fraction and properties of bars measured from the data are affected by systematic effects such as cosmological dimming, loss of spatial resolution, and band-shifting. We gauge the impact of these effects through simulations which artificially redshift out to  $z=1.2$  the optical images of a large representative sample of 144 local bright moderately inclined ( $i < 50$ ,  $B < 12$  mag) spirals (see Fig. 1), and simulate the GOODS and GEMS observations of the redshifted images taking into account background, readnoise, instrumental/filter response, and exposure time (see Fig. 2).

## GALAXY FITTING AND NUMERICAL MODELLING

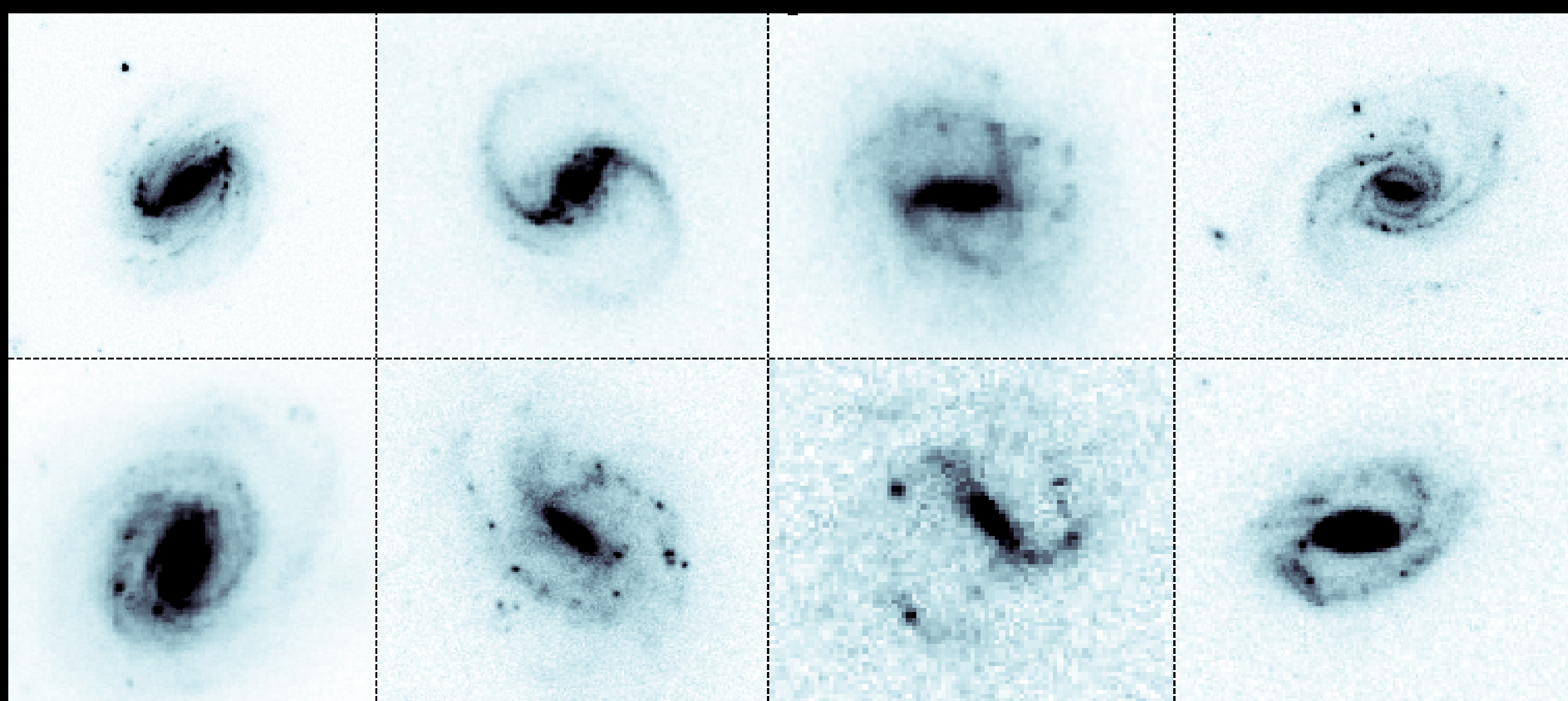


FIG. 3 - Bars at  $z=0.2-1$ : The superb GEMS and GOODS images of barred spirals at  $z=0.2-1$  have a sampling resolution of  $0.05''$  corresponding to 300 pc at  $z=0.5$  and 400 pc at  $z=1$ , for a flat cosmology with a Hubble constant of 70 km/s per Mpc and  $\Omega_{\Lambda} = 0.7$ .

- Bars are characterized in the local sample and in the GOODS and GEMS surveys (Fig. 3) using an automated version of the STSDAS ellipse routine (Fig. 4) and GALFIT (Peng et al. 2002).
- We also investigate via simulations and numerical modelling environmental effects and internal dynamics which influence the bar fraction at intermediate redshifts: **(1) Interactions:** Equal mass mergers tend to produce violent relaxation while moderate mergers and weak tidal interactions can easily excite bars and spirals in a dynamically cold disk. **(2) High rates of bar destruction** at  $z > 0.5$  have been invoked to explain a low bar fraction. However, bar destruction leaves behind dynamically hot disks which cannot be trivially cooled enough to reproduce the high bar fraction at  $z=0$ . **(3) Triaxial and centrally concentrated halos** which are typical of CDM models with baryons tend to delay bar and disk formation to lower redshifts due to their orbital structure (Fig. 5).

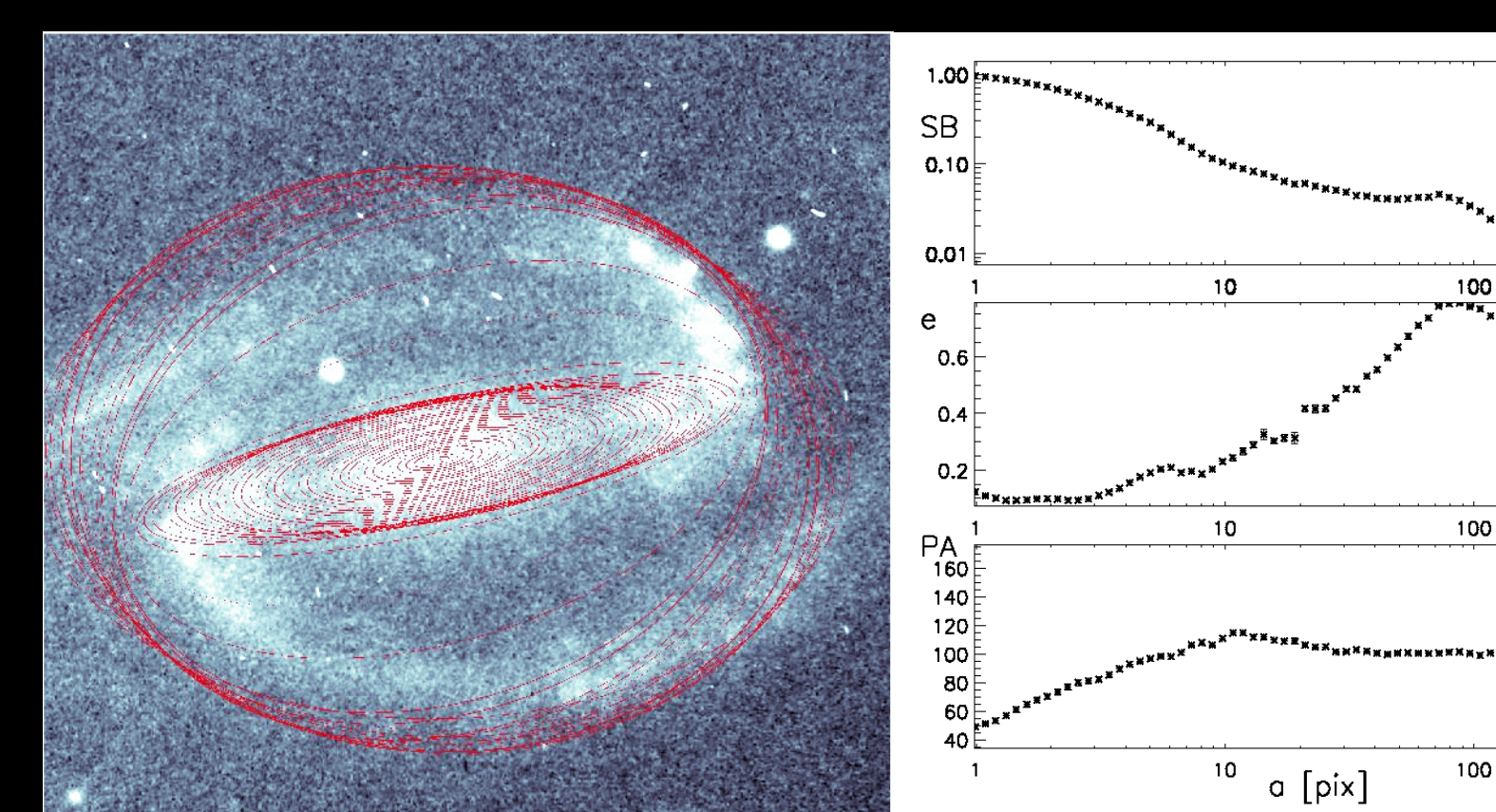


FIG. 4 - Ellipse fits: Example of ellipse fitting (left) to identify stellar bars. The peak in ellipticity over a plateau in position angle (right) is a characteristic bar signature, reflecting the dominant  $x_1$  family of stellar orbits.

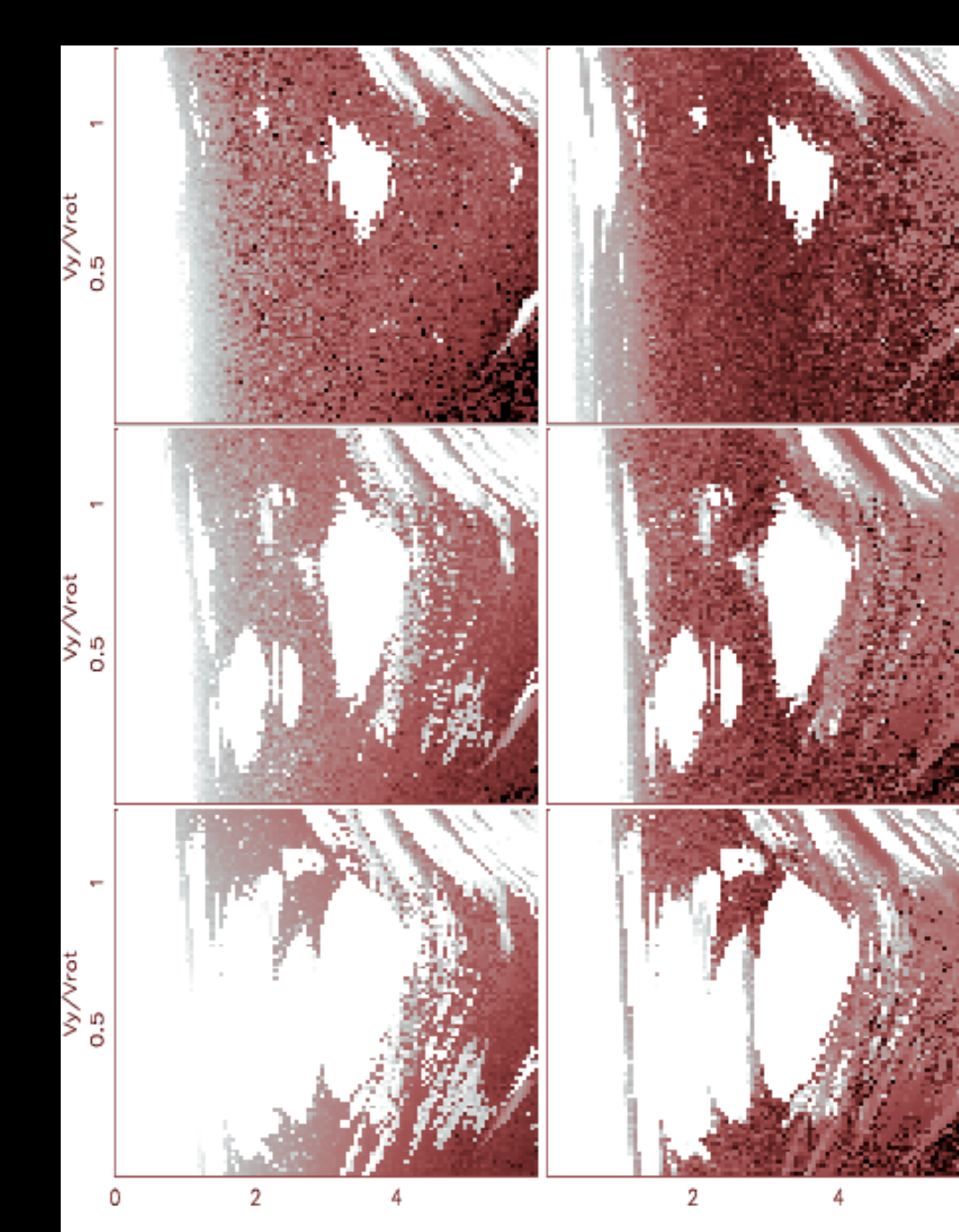


FIG. 5 - The effect of triaxial halos on bar stability: The stability of a stellar bar (with semimajor axis 6 kpc) embedded in a centrally-concentrated CDM halo decreases for lower halo axial ratios (1.0= lower, 0.99= middle, 0.95= top panels). The x-axis is the distance along the bar major axis in kpc. The y-axis is the rotational velocity in units of local rotational velocity. White shades represent regular orbits comprising the bar while red shades represent chaotic orbits. Notice that bars embedded within halos of even moderate triaxiality are profoundly unstable on dynamical timescales (El-Zant & Shlosman 2002).